ResearchGate

See discussions, stats, and author profiles for this publication at: https://www.researchgate.net/publication/349739122

Synthesis, characterization, and photocatalytic activity of ZnS and Mn-doped ZnS nanostructures

Article *in* MRS Advances · March 2021

DOI: 10.1557/s43580-021-00035-y

CITATIONS
11

READS
91

8 authors, including:

Josian Luciano Velázquez
University of Puerto Rico at Ponce
6 PUBLICATIONS **20** CITATIONS
SEE PROFILE

Yan Xin
Florida State University
234 PUBLICATIONS **7,006** CITATIONS
SEE PROFILE

Carla Quiles
University of Puerto Rico at Mayagüez
1 PUBLICATION **11** CITATIONS
SEE PROFILE

Sebastián A. Cruz-Romero
University of Puerto Rico at Mayagüez
2 PUBLICATIONS **11** CITATIONS
SEE PROFILE

All content following this page was uploaded by Josian Luciano Velázquez on 21 May 2024.

The user has requested enhancement of the downloaded file.

MRS Advances

Synthesis, Characterization, and Photocatalytic Activity of ZnS and Mn-doped ZnS Nanostructures

Josian Luciano-Velázquez[1], Yan Xin[2], Yi-feng Su[2], Carla I. Quiles-Vélez[1], Sebastián A. Cruz-Romero[1], Gabriel E. Torres-Mejías[3], Julio Rivera-De Jesús[1], and Sonia J. Bailón-Ruiz[3*]

[1] *University of Puerto Rico at Mayagüez, Mayagüez, P.R. 00681-9000*

[2]*National High Magnetic Field Laboratory, Florida State University, 1800 E. Paul Dirac Drive. Tallahassee, FL 32310-37063*

[3]*Department of Chemistry and Physics, University of Puerto Rico in Ponce, Ponce, P.R. 00716*

Abstract:
Semiconductor quantum dots like zinc sulfide have interesting potential applications, consequent to their size-dependent optical properties. These nanostructures can be used on agriculture, environmental chemistry, fluorescence microscopy, and among others. The great rise in nanotechnology has sparked the scientific community's interest in nanomaterials for the use of photodegradation in aquatic bodies. Quantum Dots (QDs) like ZnS nanoparticles (NPs) can absorb electromagnetic radiation and generate photo-excited nanostructures which would be generating reactive oxygen species (ROS) directly in aqueous phase. The presence of ROS in aquatic environments can be used to destroy organic contaminants by photocatalysis processes. Previous studies had evidenced that the presence of impurities (i.e. copper, manganese, nickel) into the crystalline structures of QDs can enhance their optical properties and consequently their catalytic capacity. Because of this, the present investigation was focused on generating water stable ZnS nanoparticles with catalytic properties. In this work, we have synthesized pure and doped ZnS nanoparticles using a reflux method; The morphology of these QDs were characterized by transmission electron microscopy (TEM); We also studied the photocatalytic properties of these nanostructures. A red shift was observed in the photoluminescence peak of pure ZnS nanoparticles when they were doped with heavy metals. Pure ZnS NPs and Mn-doped ZnS NPs showed luminescent peaks at 444 nm and 596 nm, respectively. Photodegradation studies were evaluated in presence of organic dyes like Tropaeolin O (TO) and different concentrations of quantum dots (250 ppm and 500 ppm). The photodegradation of TO was dependent of the QDs concentration and exposure time. The destruction of organic dyes in the presence of photo-excited ZnS nanoparticles is envisioned as a fast and clean technology.

**Corresponding author's detail: e-mail sonia.bailon@upr.edu (Sonia J. Bailón-Ruiz)*

INTRODUCTION:

Water pollution is a serious problem in the word, generated mainly by the residual effluents produced by Industries. Around 700,000 tons of dyes are produced annually. These are used in textile (54%), dyeing (21%), paper and pulp (10%), tanning and painting (8%), and dye manufacturers (7%) (Katheresan et al., 2018). More than 50% of the dye used is thrown in sewages and can negatively affect aquatic ecosystems. These dyes seriously affect the quality and transparency of water bodies and prevent the penetration of sunlight necessary for the process of photosynthesis in aquatic plants. Also, the depletion of dissolved oxygen in water is the most serious effect of textile waste as dissolved oxygen is very essential for marine life. These emerging contaminants have been associated with diseases as cancer, mutations, and dysfunctions. (Yusuf et al., 2015; Markandeya et al., 2017; Mani et al., 2018; Kim et al., 2020).

Tropaeolin O ($C_{12}H_9N_2NaO_5S$) (sodium-4-[(2E)-2-oxonophthalen-1-ylidene) hydrazinyl] benzenesulfonate) is used as pH indicator, coloring agent in food additives, and one of the most used dyes in fabric production globally (de Sales et al., 2015). This aromatic organic substance is extremely toxic and can irritate the skin. When being in contact with water for a long time, it can transform into carcinogenic aromatic amines. Humans are also affected because dyes can accumulate in fish tissue we later consume (Pande et al., 2019).

Photocatalysis is a photochemical process where solar energy is transformed into chemical energy on a semiconductor's surface (i.e. quantum dots) as a catalyst to accelerate the reaction's speed. The photocatalytic effect parts from eliminating organic pollutants present in water and stem from the environment's decontamination's natural principle. The most common photocatalyst is TiO_2, which is found in sun creams, aspirin, toothpaste, etc. (Sharma et al., 2019). However, this type of photocatalyst, if inhaled, at high concentrations, irritates the throat and nose, mild skin irritation, and slight irritation if in contact with the eyes. For this reason, TiO_2 classifies as a type 2 carcinogenic. Another disadvantage of the application of TiO_2 is related to its high band-gap energy. Plant peroxidases (Kalsoom et al., 2015), magnetic Fe_0 / Fe_3O_4, graphene composites (Chong et al., 2016), and microbial enzymes (Sarkar et al., 2017) are other techniques used to degrade azo dyes aromatic rings. In addition to photocatalysis, different methods work on the degradation of dyes. This includes The Fenton process that utilizes iron catalysts with H_2O_2, and Biomass, a degradation technique that uses microorganisms to produce enzymes that interact with dye molecules (Sun et al., 2018). The Fenton process has many disadvantages: 1) the formation of sludge due to large amounts of ferrous iron, and 2) the high concentration of anions in wastewater requiring neutralizing the high pH level this application causes. Biomass has drawbacks ranging from the number of tanks needed to make the system clean the system used to apply this technique. This makes it difficult to set up due to the high cost of funds, time, and maintenance required.

Photodegradation is a powerful technique that requires electromagnetic radiation to activate semiconductor nanomaterials. It generates a temporarily unstable species (electron-hole pair within the semiconductor material), this species generates Reactive oxygen species (ROS), and the ROS ends up destroying the organic compound. (Ma et al., 2019). Furthermore, nanoscale materials have higher superficial area than its counterparts (bulk); which increases the efficiency of ROS production on the nanomaterials' surface. (Sharma et al., 2019).

Quantum dots (QDs) are semiconductor nanocrystals with a size of 1 to 10 nm and have a fluorescent property that distinguishes them from the rest. (Owen & Brus, 2017). These nanostructures have piqued researchers' interest due to their unique application as an advanced oxidation process to eliminate many organic pollutants in water, such as dyes. Dye degradation using semiconductors have received much attention

due to its applications. Examples of these include TiO_2, CuS, CdSe, ZnSe, and among other. The photocatalytic reaction based in the presence of QDs is suggested to be described in five steps for the removal of pollutants: 1) diffusion of reactants to the surface of photocatalyst particles, 2) adsorption of reactants onto the surface, 3) reaction on the surface, 4) desorption of products from the surface, and 5) diffusion of products from the surface to the bulk solution (Asl, 2017). Based on the mentioned above, the objectives of this work were: i) synthesize pure and doped zinc sulphide quantum dots, ii) characterize structurally, morphologically, and optically quantum dots, iii) and evaluate the photocatalytic capacity of pure and doped quantum dots in polluted aqueous matrices.

METHODOLOGY

Synthesis of pure ZnS and Mn-doped ZnS Quantum Dots

ZnS quantum dots were synthetized by adding sodium sulfide (3% w/v) to a boiling aqueous solution of zinc sulfate (99.999% trace metals basis) 0.40 M. The reaction proceeded in a reflux system for 10 minutes until the generation of a slightly cloudy white solution. The generation of Mn-doped ZnS nanoparticles was carried out in presence of zinc sulphate, manganese sulphate 0.15 M and sodium sulfide (3 % w/v). The solution was refluxed at 100 °C for 10 minutes.

Produced nanostructures (pure and doped) were precipitated with isopropanol (HPLC grade, 99.5%), centrifuged for 15 min at 7500 rpm, and resuspended in deionized water for further characterization.

Characterization of Quantum Dots

The Quantum Dots' optical properties were studied by absorption and fluorescence spectroscopy using a JASCO 6000 Spectrophotometer and a Shimadzu RF-6000 Spectrofluorometer, respectively. The Quantum Dots' morphology was evaluated using TEM on a JEOL JEM-ARM200cF microscope at 200kV, which is equipped with Oxford Aztec energy dispersive X-ray spectrometer.

Photodegradation of Tropaeolin O

The photodegradation capacity of pure (ZnS) and doped (Mn-doped ZnS) nanostructures were studied in presence of cationic dyes as 40.0 µM-Tropaeolin O, at room temperature. Purified nanostructures were evaluated at concentrations of 250 ppm and 500 ppm. An 8 watt-UV lamp was used as the irradiation source with a power irradiation of 10 mW. cm^{-2}. Dyes were contacted with pure and doped nanostructures at time intervals of 0, 15, 30, 60, 90, 120, and 150 minutes under constant agitation (20 rpm) and 302 nm-UV irradiations. Aliquots of the photodegraded solutions were monitored under absorbance spectroscopy at 426 nm for Tropaeolin O. The decrease in the dyes' concentration of the dyes over time was estimated from calibration curves previously prepared. In this way, absorbance calibration curves for Tropaeolin O at concentrations ranging from 1 µM to 50 µM were plotted and the line equation and correlation coefficients were determined.

For comparison purposes, the degradation of Tropaeolin in absence of nanostructures was evaluated under darkness or under 302 nm- electromagnetic irradiation.

RESULTS AND DISCUSSION

Optical properties of Quantum Dots

UV-Vis analyses, shown in Figure 1, evidences the presence of shoulders centred approximately on 303 nm for both pure ZnS and Mn-doped ZnS, respectively, which corresponds to the excitonic peak in Zinc-based nanostructures. The band gap energy of pure and doped ZnS was estimated, using Tauc's relationship, at 3.70 eV that suggests the quantum confinement effect (ZnS bulk, 3.6 eV). The fluorescence spectra for pure and doped QDs are shown in Figure 2. For ZnS a broad peak is observed around 444 nm (blue range) which is attributed to the presence of defects on the quantum dots surface. Doped nanoparticles evidenced two peaks. The first centred at 444 nm and the second at 596 nm. The substitution of $Mn^{2+}(3d^5)$ ions into the Zn^{2+} $(3d^{10})$ sites generates the presence of a second emission peak in the orange range at 596 nm.

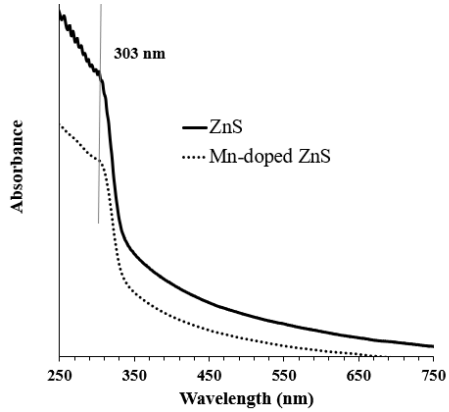

Figure 1: Absorbance Spectra for pure and Mn-doped ZnS Quantum Dots

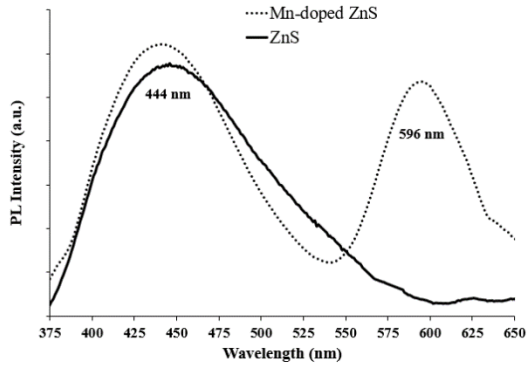

Figure 2: Photoluminescence Spectra for pure and Mn-doped ZnS Quantum Dots

Morphology, Structural, and Composition of Quantum Dots

The morphology of pure ZnS QDs is shown in Figure 3. The average size is around 4 nm. The energy dispersive X-ray spectroscopy (EDS) studies (Figure 3d) confirmed the elemental composition of the nanoparticles with 52.26% and 47.74% of Zinc and Sulphur respectively. Other peaks (as copper) proceed from TEM grid. Electron diffraction pattern (Figure 3b) confirms that the nanoparticles have a fcc zinc-blende cubic structure with the most prominent concentric rings, which correspond to the crystalographic planes (111), (220). The high resolution TEM (HRTEM) image confirms the crystallinity of the QDs (Figure 3c).

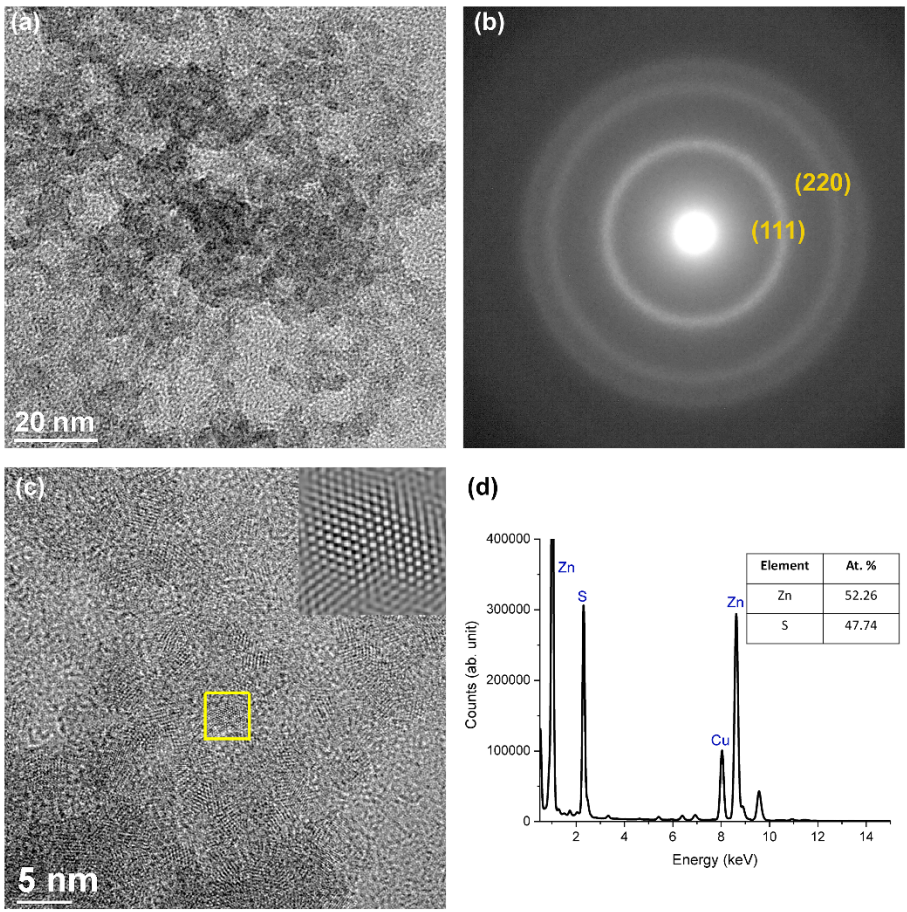

Figure 3: TEM characterization of pure ZnS QDs. (a)Low magnification TEM image of the QDs. (b) electron diffraction pattern of those ZnS nanoparticles; (c)HRTEM image of the nanoparticles. Inset: FFT filtered image of the boxed particle viewed along [111]. (d) EDS spectrum of the nanoparticles.

Figure 4 shows some evidence of the presence of manganese into the ZnS structures. For the Mn-doped ZnS QDs, the diameter of the nanoparticle size does not change, and it is still around 4 nm. The EDS analysis (Figure 4d) indicates that there might be a very small amount of Mn in the sample of about 0.22 at.%. Doped samples also showed 56.31 % of zinc and 43.48 % of sulphur. The other peaks are spurious X-ray from sample holder and TEM grid. The ED pattern and HRTEM (Figure 4b and 4c) confirm that nanoparticles doped with manganese have the same FCC crystalline structures.

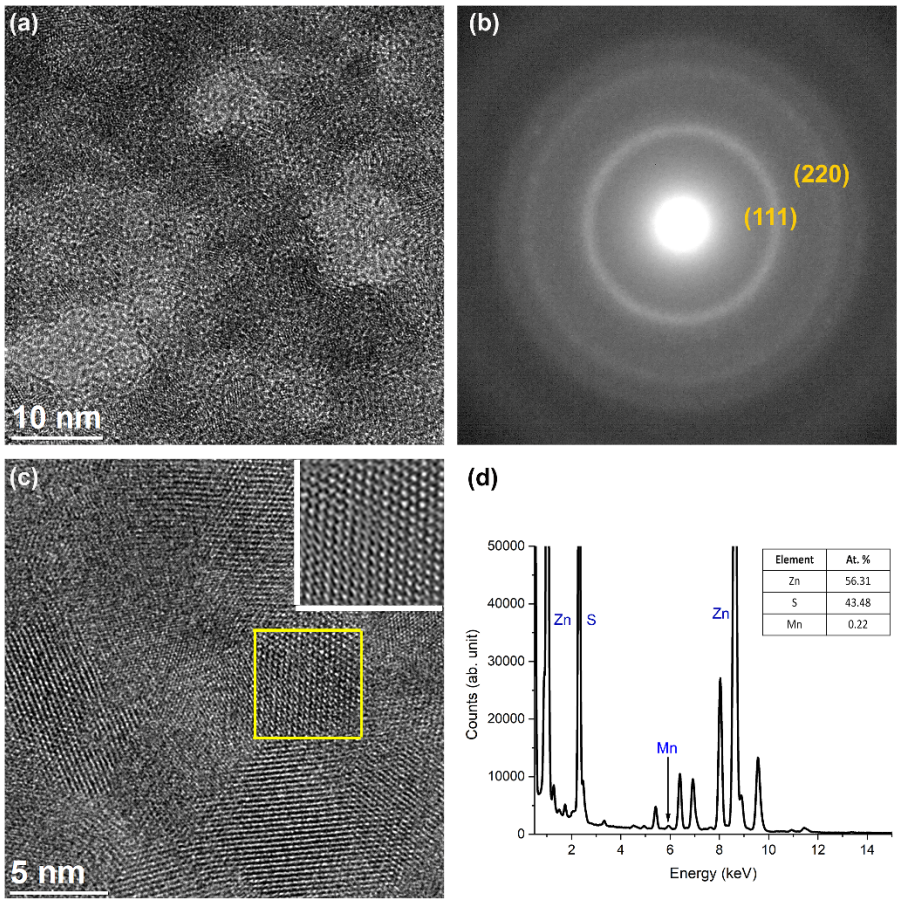

Figure 4: TEM characterization of Mn-doped ZnS QDs. (a)Low magnification TEM image of the QDs. (b) electron diffraction pattern of those ZnS nanoparticles; (c)HRTEM image of the nanoparticles. Inset: FFT filtered image of the boxed particle viewed along [111]. (d)EDS spectrum of the nanoparticles.

Photodegradation of Tropaeolin O

Pure and doped ZnS Quantum dots were used to evaluate their catalytic capacity to degrade Tropaeolin O. A calibration curve was carried out using standards solution of Tropaeolin O from 1 µM to 50 µM. Figure 5 shows the variation of the relative dye concentration (*Cf*/*Ci*) with UV-irradiation time for Tropaeolin O (TO) in presence of 250 ppm and 500 ppm of pure and Mn-doped QDs. The process was dependent on QDs concentration and the UV-irradiation time. The control groups (UV light and Darkness) do not suffer degradation during the tested period (0 to 150 minutes), which indicates that the decrease in the TO concentration is only due to photo-degradation by the quantum dots. The TO (initial concentration of 40 µM) degradation percentages were 87.7% and 92.6 % when irradiated for 30 minutes with UV light at 302 nm, using 250 ppm and 500 ppm of pure ZnS QDs, respectively. The trends observed can be attributed to the increase of the number of active photocatalytic sites at larger quantities of nanoparticles (500 ppm) suspended in the irradiated volume. For the same irradiation time (30 minutes), the degradation percentages for TO were 40.4% and 47.5% respectively, in presence of 250 ppm and 500 ppm of doped structures. It can be observed that in photocatalysis initial stages, pure nanostructures are more efficient than doped nanoparticles. However, at 90 minutes of treatment, pure and doped QDs achieved a maximum photodegradation of 94% of tropaeolin O. The degradation of Tropaeolin O in presence of QDs could be due to the production of ROS (as hydroxyl radicals) in the aqueous media when QDs are activated by electromagnetic radiation at 302 nm.

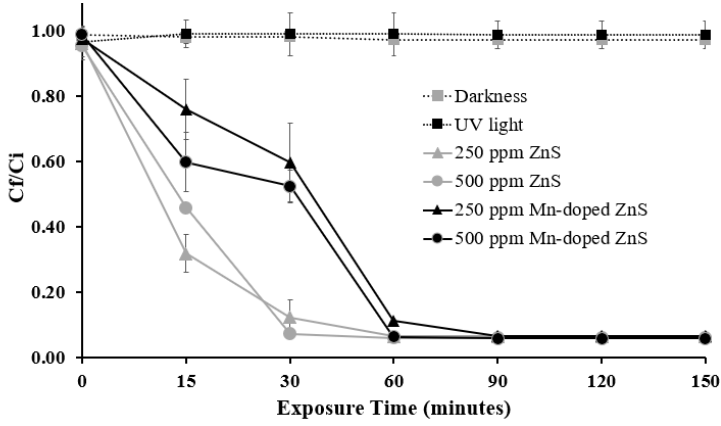

Figure 5: Photodegradation of Tropaeolin O in presence of pure ZnS and Mn-doped ZnS Quantum Dots

CONCLUSION

ZnS nanoparticles (pure and Mn-doped) were synthesized in aqueous media and evidenced diameters less than 5 nm. Nanostructures showed face-centered cubic arrangements and the elemental composition was confirmed by energy dispersive X-ray studies. A main emission peak centered at 444 nm was found for ZnS nanoparticles. The presence of manganese at trace concentration into the ZnS crystalline red generated a second peak at 596 nm. The photodegradation capacity of quantum dots (pure and Mn-doped) was dependent of the QDs concentration. In this way, at 30 minutes of treatment, both type of nanoparticles at concentrations of 500 ppm were more efficient than its counterparts at 250 ppm. Furthermore, both quantum dots (pure and Mn-doped) were able to degrade tropaeolin O almost completely (94%) after 90 minutes of photocatalysis.

ACKNOWLEDGEMENTS

This work was supported by Institutional funds of Dr. Sonia J. Bailon-Ruiz of the UPRP. We carried out this research thanks to the collaboration of the following people and programs. Thanks to Dr. Tessie H. Cruz-Rivera (Rector of the UPRP) for allowing us to use the facilities and always supporting us in the process. Thanks to Dr. Milton Rivera-Ramos (Department Chair of Chemistry and Physics, UPRP), the Department of Biology, Dr. Pier Le Compte-Zambrana, Dr. Luis Alamo-Nole (Associate Professor, PUCPR), Puerto Rico Louis Stokes Alliance for Minority Participation (PR-LSAMP) and the UPRM.

TEM work was performed at the National High Magnetic Field Laboratory, which is supported by National Science Foundation Cooperative Agreement No. DMR-1644779* and the State of Florida.

References

[1] Asl, S. **6**, 65-72 (2017).
[2] Chong, S., Zhang, G., Tian, H., and Zhao, H. **44**, 148-157 (2016).
[3] de Sales, P. F., Magriotis, Z. M., Rossi, M. A. L. S., Resende, R. F., and Nunes, C. A. **151**, 144-152 (2015).
[4] Fakhri, A., Azad, M., and Tahami, S. **28**, 16397–16402 (2017).
[5] Ibarbia, A., Grande, H. J., and Ruiz, V. **37**, 5 (2020).
[6] Kalsoom, U., Bhatti, H. N., and Asgher, M. **176**, 1529-1550 (2015).
[7] Katheresan, V., Kansedo, J., and Lau, S. Y. **6**, 4676-4697 (2018).
[8] Kim, S., Lee, J., Son, Y., and Yoon, M. **41**. 843-850 (2020).
[9] Ma, H.-Y., Zhao, L., Guo, L.-H., Zhang, H., Fengjie, C., and Yu, W. **369**, 719-726 (2019).
[10] Mani, S., Chowdhary, P., and Bharagava, R. **92**, 1844-1849 (2018).
[11] Markandeya, Dhiman, N., Shukla, S. P., and Kisku, G. C. **149**, 597–606 (2017).
[12] Owen, J., and Brus, L. **32**, 10939-10943 (2017).
[13] Pande, V., Pandey, S., Joshi, T., Sati, D., Gangola, S., Kumar, S., and Samant, M. 255-287 (2019).
[14] Pirsaheb, M., Asadi, A., Sillanpää, M., and Farhadian, N. 857-871 (2018).
[15] Sarkar, S., Banerjee, A., Halder, U., Biswas, R., & Bandopadhyay, R. **4**, 121-131 (2017).
[16] Shakoor Sadia A4 - Nasar, Abu, S. A.-S. **5**, 152-159 (2017).
[17] Sharma, K., Dutta, V., Sharma, S., Raizada, P., Hosseini-Bandegharaei, A., Thakur, P., and Singh, P. **78**, 1-20 (2019).
[18] Sun, Q., Hong, Y., Liu, Q., and Dong, L. *430*, 399–406 (2018).
[19] Teixeira, S., Martins, P. M., Lanceros-Méndez, S., Kühn, K., and Cuniberti, G. **384**, 497-504 (2016).
[20] Yusuf, M., Elfghi, F. M., Zaidi, S. A., Abdullah, E. C., and Khan, M. A. **5**, 50392 (2015).
[21] YW, Q., LF, Z., Shen, X., Sotto, A., CJ, G., and JN, S. **222,** 117-124 (2019).

View publication stats